4854 *Organometallics* 1993, *12*, 4854-4862

Fe_3–Triangle Opening and Closing by a Single Two-Electron Process: Role of the One-Electron-Reduced Intermediate in the Electrocatalytic Ligand Substitution Reactions of $Fe_3(CO)_9(\mu_3\text{-}PMn(CO)_2Cp)_2$

Yoshihiro Koide and Cynthia K. Schauer*

Department of Chemistry, The University of North Carolina at Chapel Hill,
Chapel Hill, North Carolina 27599-3290

Received September 22, 1993[⊗]

The radical $[Fe_3(CO)_9(\mu_3\text{-}PMn(CO)_2Cp)_2]^{\bullet-}$ ($1^{\bullet-}$) is implicated as the active species in the electron-transfer-chain (ETC) catalytic ligand substitution of the Fe-bound carbonyl ligands in $Fe_3(CO)_9(\mu_3\text{-}PMn(CO)_2Cp)_2$ (1). $1^{\bullet-}$ is the 1-e^- reduced intermediate relating the closed cluster 1 (with three Fe–Fe bonds) and the open cluster 1^{2-} (with two Fe–Fe bonds); interconversion between 1 and 1^{2-} occurs in a single 2-e^- wave (ΔE_p = 36 mV) in the cyclic voltammogram. Substitution of CO by $P(OMe)_3$ or PMe_3 can be induced by passing a small amount of cathodic current while a cyclic voltammogram is acquired in the presence of PR_3 to sequentially produce $Fe_3(CO)_8(PR_3)(\mu_3\text{-}PMn(CO)_2Cp)_2$ (11, R = OMe; 12, R = Me) and then $Fe_3(CO)_7(PR_3)_2(\mu_3\text{-}PMn(CO)_2Cp)_2$ (21, R = OMe; 22, R = Me); no tris-substituted clusters are observed under electrocatalytic conditions. The sequential substitutions of CO by PR_3 occur on two different $Fe(CO)_3$ groups. The 2-e^- behavior observed for 1 is maintained in the PR_3-substituted derivatives. The same clusters can also be produced on a preparative scale in THF solution using a catalytic amount of sodium benzophenone ketyl to initiate the radical chain in the presence of the appropriate stoichiometric amount of PR_3. Reactions between 1^{2-} and PR_3 can be induced by oxidative electrochemistry, but the reactions are not electrocatalytic. The efficiency of the ETC reaction was gauged by the measurement of turnover numbers (TN) for the $P(OMe)_3$ substitution reaction. The first step proceeds with a TN of ~1000 mol/faraday while TN for the second substitution step drops to ~100 mol/faraday. The substitution reaction rate is insensitive to the nature and concentration of the incoming nucleophile, and the reaction is strongly inhibited by a CO atmosphere, all consistent with a CO-dissociative mechanism. The isolated PR_3-substituted clusters are unstable to bulk reduction. The monosubstituted clusters undergo a rapid, clean disproportionation reaction that is induced by a ligand redistribution corresponding to the net reaction 11 (or 12) + $1e^- \rightarrow {}^1/_2 1^{2-} + {}^1/_2 21$ (or 22).

Introduction

Electrochemical studies have played a prominent role in the study of the multiple redox states of transition metal clusters.[1] Odd-electron clusters, generated electrochemically, chemically, or photochemically often display enhanced reactivity toward ligand substitution and other chemical reactions.[2] Such enhanced reactivity has enabled facile, selective substitution of CO for donor ligands in many inert transition metal carbonyl clusters via a *reductive* electron-transfer-chain (ETC) catalytic pathway (Scheme I).[3-10] In this scheme the electron is the catalyst and the net reaction ($M_x(CO) + L \rightarrow M_xL + CO$) does not involve a change in redox state.[3] The basic requirement for an efficient reductive catalytic cycle is that the ligand-substituted product, M_xL, has a more negative reduction potential than the starting material, $M_x(CO)$. This

---

[⊗] Abstract published in *Advance ACS Abstracts,* November 1, 1993.

(1) For reviews, see: (a) Geiger, W. E.; Connelly, N. G. *Adv. Organomet. Chem.* 1985, *24,* 87. (b) Geiger, W. E. *Prog. Inorg. Chem.* 1985, *33,* 275. (c) Lemoine, P. *Coord. Chem. Rev.* 1988, *83,* 169. (d) Drake, S. R. *Polyhedron* 1990, *9,* 455. (e) Lemoine, P. *Coord. Chem. Rev.* 1982, *47,* 55.

(2) (a) Chanon, M. *Acc. Chem. Res.* 1987, *20,* 214. (b) *Organometallic Radical Processes*; Trogler, W. C., Ed.; Elsevier: New York, 1990; see also references therein.

(3) For reviews of organometallic electron transfer chain catalysis see: (a) Astruc, D. *Angew. Chem., Int. Ed. Engl.* 1988, *27,* 643. (b) Coville, N. J. In ref 2b, p 108. (c) Kotz, C. In *Paramagnetic Organometallic Species in Activation, Selectivity, and Catalysis*; Chanon, M., Juillard, M., Poite, J. C., Eds.; NATO ASI Series; Kluger Academic: Dordrecht, The Netherlands 1989; p 171.

(4) Bezems, G. J.; Rieger, P. H.; Visco, S. *J. Chem. Soc., Chem. Commun.* 1981, 265.

(5) $Fe_3(CO)_9(\mu_3\text{-}E)_2$ clusters: (a) Darchen, A.; Mahé, C.; Patin, H. *J. Chem. Soc., Chem. Commun.* 1982, 243. (b) Darchen, A. *Nouv. J. Chim.* 1982, *6,* 539. (c) Ohst, H. H.; Kochi, J. K. *J. Am. Chem. Soc.* 1986, *108,* 2897. (d) Bockman, T. M.; Kochi, J. K. *J. Am. Chem. Soc.* 1987, *109,* 7725.

(6) $Co_3(CO)_9(\mu_3\text{-}CR)$ clusters: (a) Hinkelmann, K.; Heinze, J.; Schacht, H.; Field, J. S.; Vahrenkamp, H. *J. Am. Chem. Soc.* 1989, *111,* 5078. (b) Downard, A. J.; Robinson, B. H.; Simpson, J. *Organometallics* 1986, *5,* 1140. (c) Downard, A. J.; Robinson, B. H.; Simpson, J. *Organometallics* 1986, *5,* 1132. (d) Downard, A. J.; Robinson, B. H.; Simpson, J. *Organometallics* 1986, *5,* 1122.

(7) $Co_4(CO)_{10}(\mu_4\text{-}PPh)_2$: (a) Richmond, M. G.; Kochi, J. K. *Organometallics* 1987, *6,* 254. (b) Richmond, M. G.; Kochi, J. K. *Inorg. Chem.* 1986, *25,* 656.

(8) (a) Bruce, M. I.; Kehoe, D. C.; Matisons, J. G.; Nicholson, B. K.; Rieger, P. H.; Williams, M. L. *J. Chem. Soc., Chem. Commun.* 1982, 442. (b) Bruce, M. I.; Matisons, J. G.; Nicholson, B. K.; Williams, M. L. *J. Organomet. Chem.* 1982, *236,* C57. (c) Lahuerta, P.; Latorre, J.; Sanau, M.; Kisch, H. *J. Organomet. Chem.* 1985, *286,* C27. (d) Rimmelin, J.; Lemoine, P.; Gross, M.; Bahsoun, A. A.; Osborn, J. A. *Nouv. J. Chim.* 1985, *9,* 181.

(9) Examples of dinuclear systems: (a) Lhadi, E. K.; Mahé, H.; Patin, H.; Darchen, A. *J. Organomet. Chem.* 1983, *246,* C61. (b) Lhadi, E. K.; Patin, H.; Darchen, A. *Organometallics* 1984, *3,* 1128. (c) Darchen, A.; Lhadi, E. K.; Patin, H. *J. Organomet. Chem.* 1983, *259,* 189. (d) Schroeder, N. C.; Angelici, R. J. *J. Am. Chem. Soc.* 1986, *108,* 3688.

(10) Initiation of an ETC chain by generation of a 19-electron species following photolytic cleavage of metal carbonyl dimers has been reported: (a) Stiegman, A. E.; Tyler, D. R. *Comments Inorg. Chem.* 1986, *5,* 215. (b) Stiegman, A. E.; Goldman, A. S.; Leslie, D. B.; Tyler, D. R. *J. Chem. Soc., Chem. Commun.* 1984, 632. (c) Goldman, A. S.; Tyler, D. R. *Inorg. Chem.* 1987, *26,* 253.

0276-7333/93/2312-4854$04.00/0

requirement is satisfied by any substitution reaction that replaces a π-acid CO ligand by a phosphine donor. The radical chain is propagated by an electron transfer reaction between $M_xL^{\bullet-}$ and $M_x(CO)$ to regenerate $M_x(CO)^{\bullet-}$ (eq 3).

Scheme I

$$\text{initiation} \qquad M_x(CO) \xrightarrow{e^-} M_x(CO)^{\bullet-} \qquad (1)$$

$$\text{propagation} \qquad M_x(CO)^{\bullet-} + L \rightarrow M_xL^{\bullet-} + CO \qquad (2)$$

$$M_xL^{\bullet-} + M_x(CO) \rightarrow M_xL + M_x(CO)^{\bullet-} \qquad (3)$$

We recently reported that the triiron cluster $Fe_3(CO)_9(\mu_3\text{-}PMn(CO)_2Cp)_2$ (1), with three Fe–Fe bonds, undergoes a reversible composite 2-e⁻ reduction ($E_{1/2} = -0.861$ V vs Ag/0.1 M $AgNO_3$ in CH_3CN) that is accompanied by opening of the Fe_3 triangle (eq 4).[11] The 1-e⁻-reduced intermediate, $1^{\bullet-}$, is observed in an infrared spectroelectrochemical experiment in THF solution, clearly establishing that the transformation from 1 to 1^{2-} occurs in two consecutive 1-e⁻ steps (eq 5). In CH_3CN solution, the

$$1 \overset{E^{\circ\prime}_1}{\rightleftharpoons} 1^{\bullet-} \overset{E^{\circ\prime}_2}{\rightleftharpoons} 1^{2-} \qquad (5)$$

radical is present in a sufficiently small concentration that it is not spectroscopically observable. We report here the activity of $1^{\bullet-}$ in an ETC catalytic ligand substitution reaction to produce mono- and bis-PR_3-substituted products. This is the first example of a thermodynamically unstable 1-e⁻-reduced intermediate in a well-characterized 2-e⁻ redox reaction participating in an ETC reaction.

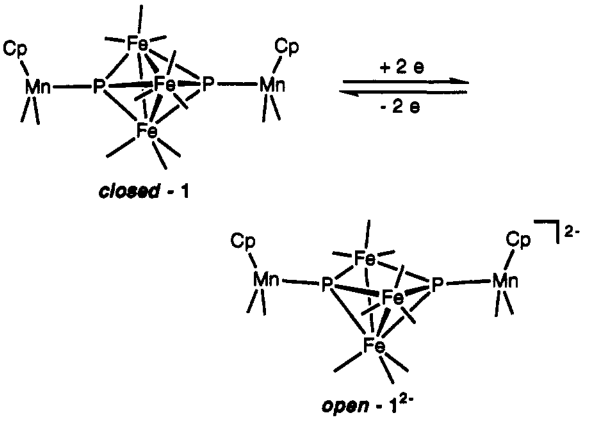

(4)

Results and Discussion

Cyclic Voltammetry. Reactions of 1 with $P(OMe)_3$ and PMe_3 were initially undertaken to determine the influence of the substitution of CO by phosphine on the two 1-e⁻ potentials comprising the 2-e⁻ wave. A representative set of successive cyclic voltammograms of 1 in CH_3CN solution taken in the presence of 80 equiv of added ligand is shown in Figure 1 for $P(OMe)_3$. With increasing number of CV cycles, a new reversible reduction peak ($E_{pc} = -1.133$ V) appears at a potential 0.25 V more negative than the potential for 1 ($E_{pc} = -0.879$ V), indicating a substitution reaction is occurring in the *bulk solution*.[12]

The apparent isopotential points observed at −1.09 and −0.87 V for the cathodic and the anodic scans, respectively, are interpreted analogously to isosbestic points and demonstrate that the substitution reaction proceeds without side reactions. Neither 1 nor 1^{2-} undergoes phosphine substitution for CO in CH_3CN solution over a period of 15 h;[13] thus the electrochemically-generated 49-electron radical monoanion, $1^{\bullet-}$, is implicated as the substitutionally labile species. Infrared spectra of the electrolyte solutions following complete conversion to the new product show a pattern of CO stretching frequencies shifted to lower energy (Figure 2 and Table I show infrared data for authentic samples). Comparisons of infrared and cyclic voltammetry data to those of authentic samples of monosubstituted products (see below) confirm that simple replacement of CO by phosphine has taken place (eq 6).[14]

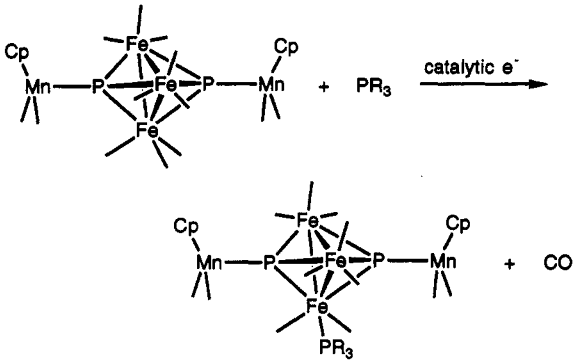

(6)

11: R = OMe
12: R = Me

The reduction potential for the PMe_3 derivative **12** is shifted by ~30 mV to more negative potentials compared to that for **11**, consistent with PMe_3 being a better donor than $P(OMe)_3$. The larger phosphine, PPh_3, does not react with $1^{\bullet-}$ in the same fashion as $P(OMe)_3$ and PMe_3, presumably due to steric crowding in the substituted product. The results of the cyclic voltammetry experiments are collected in Table II.

Once substitution of the first CO ligand is essentially complete, substitution of a CO ligand in **11** (and **12**) by another PR_3 ligand takes place (eq 7). This is evidenced by a new cathodic peak that appears an additional 0.25 V to more negative potentials (see Figure 1; $E_{pc} = -1.385$ V). Apparent isopotential points are also observed for the second substitution reaction. The shift in reduction

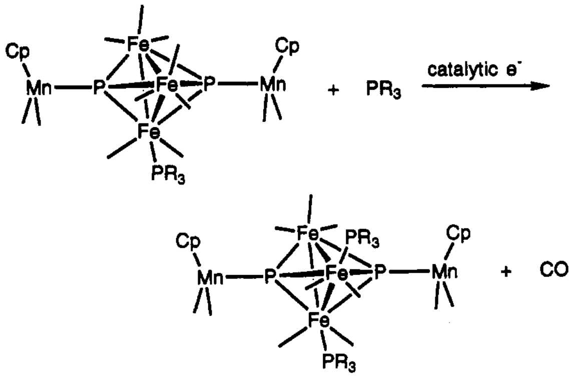

(7)

21: R = OMe
22: R = Me

---

(11) Koide, Y.; Bautista, M. T.; White, P. S.; Schauer, C. K. *Inorg. Chem.* **1992**, *31*, 3690.

(12) The shape of the 2-e⁻ anodic wave for the PR_3-substituted clusters is distorted compared to that for 1. This aspect will be discussed in detail in a future contribution.

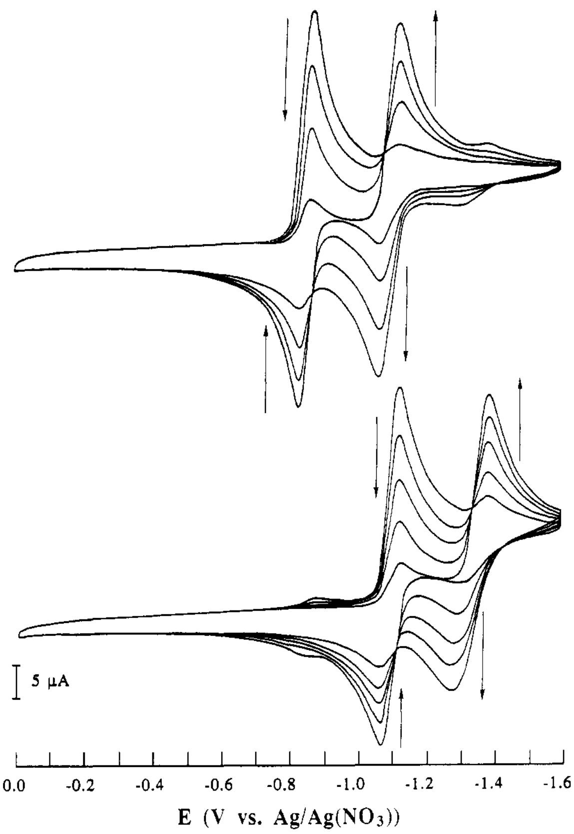

Figure 1. A set of every fourth successive cyclic voltammogram (scan rate = 50 mV s^{-1}) observed for a 1.2 mM solution of **1** in 0.1 M [(n-Bu)$_4$N][BF$_4$]/CH$_3$CN containing 80 equiv of P(OMe)$_3$ showing conversion (a, top) from **1** to **11** and (b, bottom) from **11** to **21**.

potential of ~0.25 V with each substitution of P(OMe)$_3$ for CO agrees well with the trend observed for the related cluster Fe$_3$(CO)$_9$(μ_3-PPh)$_2$ and its phosphite-substituted derivatives.[5c] Infrared spectroscopy on the electrolyte solution at the end of the reaction shows further lowering of the CO stretching frequencies for the bis-substituted products as expected (Figure 2 shows the spectrum for **21**). The observed IR spectra and cyclic voltammograms agree well with those for authentic samples of bis-substituted clusters. Upon scanning to more negative potentials, no substitution of a third P(OMe)$_3$ or PMe$_3$ ligand is observed. The steric bulk of the two capping CpMn(CO)$_2$ groups may impose difficulties for the coordination of three PR$_3$ ligands to the *closed*-Fe$_3$ array. It is noteworthy that the only cluster of the same general structural type as **1** that contains three coordinated PR$_3$ ligands is missing one CpMn(CO)$_2$ cap (eq 8).[15]

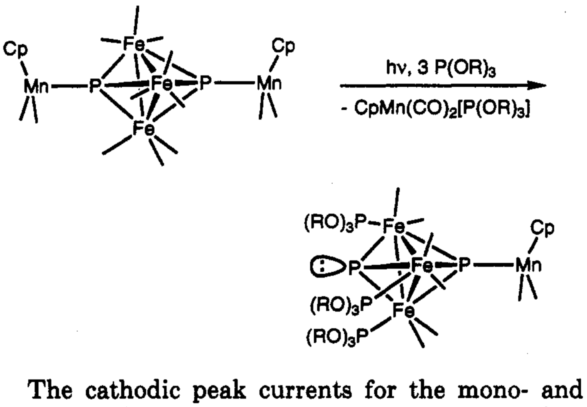

(8)

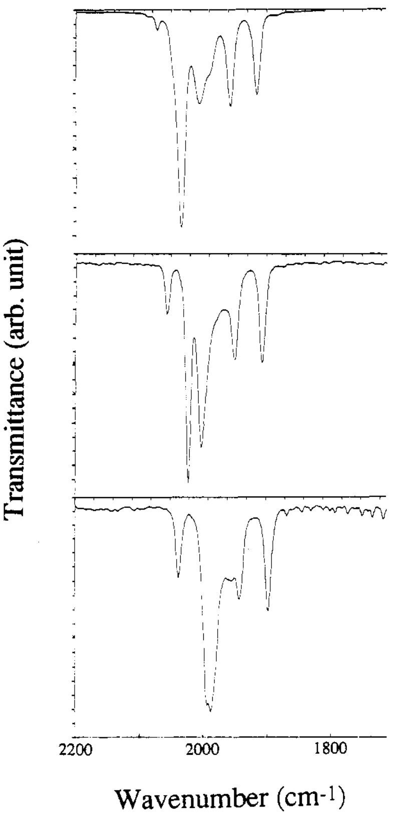

Figure 2. Infrared spectra in the CO stretching region of authentic samples of **1** (top), **11** (middle), and **21** (bottom) in THF solution.

Table I. Infrared CO Stretching Frequencies for Bicapped Triiron Clusters

cluster	ν(CO) (THF; cm^{-1})[a]
Fe$_3$(CO)$_9$(μ_3-PMn(CO)$_2$Cp)$_2$ (**1**)	2073 (w), 2036 (s), 2007 (m), 1959 (m), 1915 (m)
Fe$_3$(CO)$_8$[P(OMe)$_3$](μ_3-PMn(CO)$_2$Cp)$_2$ (**11**)	2057 (w), 2024 (s), 2002 (s), 1950 (m), 1903 (m)
Fe$_3$(CO)$_7$[P(OMe)$_3$]$_2$(μ_3-PMn(CO)$_2$Cp)$_2$ (**21**)	2037 (m), 1988 (s, br), 1943 (m), 1897 (m)
Fe$_3$(CO)$_8$(PMe$_3$)(μ_3-PMn(CO)$_2$Cp)$_2$ (**12**)	2051 (w), 2017 (s), 1998 (s), 1948 (m), 1903 (m)
Fe$_3$(CO)$_7$(PMe$_3$)$_2$(μ_3-PMn(CO)$_2$Cp)$_2$ (**22**)	2027 (w), 1975 (s), 1943 (m), 1890 (m)

[a] Legend: s = strong; m = medium; w = weak; br = broad.

The cathodic peak currents for the mono- and bis-substituted derivatives are approximately equal to that for **1**, implying that 2-e$^-$ behavior is maintained in the substituted derivatives. The minimum ΔE_p for the substituted clusters range from 34 to 61 mV. In attempts to obtain direct proof concerning the involvement of two electrons in the single waves for the ligand-substituted products using coulometry, difficulties were encountered with stability of the reduced clusters on the time scale of the bulk electrolysis experiment (see below).

The initiation of a reaction in the bulk solution by the passage of cathodic current is a characteristic feature of an electron-transfer-chain (ETC) catalytic ligand substitution reaction.[3] For the specific case of ETC catalysis of a phosphine substitution reaction involving **1**, the active

---

(13) Reactions between 1 or [BzMe$_3$N]$_2$[1^{2-}] with 100 equiv of P(OMe)$_3$ in CH$_3$CN/0.1 M [(n-Bu)$_4$N][BF$_4$] show no reaction by infrared spectroscopy after 15 h.

(14) A two-digit abbreviation is used for the PR$_3$-substituted clusters. The first digit indicates the number of PR$_3$ substituents and the second digit indicates the identity of the PR$_3$ ligand.

(15) Lang, H.; Hüttner, G.; Zsolnai, L.; Mohr, G.; Sigwarth, B.; Weber, U.; Orama, O.; Jibril, I. *J. Organomet. Chem.* **1986**, *304*, 157.

Table II. Electrochemical Parameters for Two-Electron-Reduction Waves[a]

compound	E_p(anodic)[b]	E_p(cathodic)[b]	$E_{1/2}$[c]	ΔE_p[d]
$Fe_3(CO)_9(\mu_3\text{-}PMn(CO)_2Cp)_2$ (**1**)	−0.843	−0.879	−0.861	36
$Fe_3(CO)_8[P(OMe)_3](\mu_3\text{-}PMn(CO)_2Cp)_2$ (**11**)	−1.069	−1.133	−1.091	44 (34)[e]
$Fe_3(CO)_7[P(OMe)_3]_2(\mu_3\text{-}PMn(CO)_2Cp)_2$ (**21**)	−1.279	−1.385	−1.332	106 (61)[e]
$Fe_3(CO)_8(PMe_3)(\mu_3\text{-}PMn(CO)_2Cp)_2$ (**12**)	−1.103	−1.143	−1.123	40
$Fe_3(CO)_7(PMe_3)_2(\mu_3\text{-}PMn(CO)_2Cp)_2$ (**22**)	−1.372	−1.412	−1.392	40

[a] Cyclic voltammograms were recorded in CH_3CN, containing 0.1 M $[(n\text{-}Bu)_4N][BF_4]$ at 50 mV s^{-1}. [b] In volts vs Ag/0.1 M $AgNO_3$; $E_{1/2}(Cp_2Fe/Cp_2Fe^+)$ = 0.420 V). [c] Average of cathodic and anodic peak potentials (V). [d] Difference between cathodic and anodic peak potentials (mV). [e] Values in parentheses at 5 mV s^{-1}.

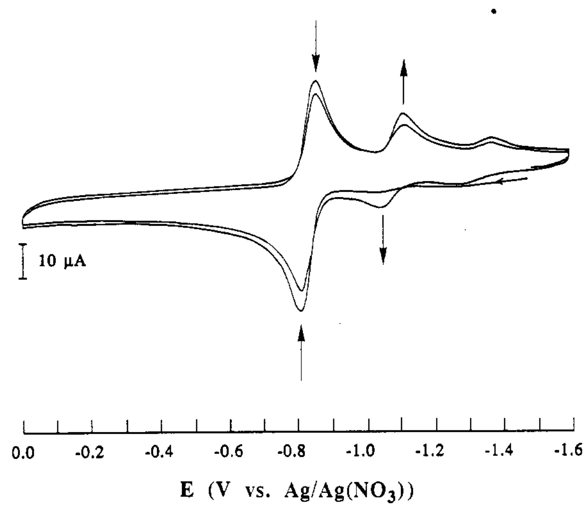

Figure 3. Cyclic voltammogram (scan rate = 50 mV s^{-1}) of 0.8 mM $[BzMe_3N]_2[1^{2-}]$ in 0.1 M $[(n\text{-}Bu)_4N][BF_4]/CH_3CN$ containing 100 equiv of $P(OMe)_3$ showing noncatalytic substitution upon oxidation.

radical, $1^{\bullet-}$, is thermodynamically unstable with respect to disproportionation, and the equilibrium radical concentration in bulk solution is governed by the disproportionation constant, K_{disp} (eqs 9 and 10).[11] The magnitude of the disproportionation constant is determined by the two 1-e⁻ potentials that comprise the composite 2-e⁻ wave at the average potential $E_{1/2} = {}^1/_2(E^{\circ\prime}{}_1 + E^{\circ\prime}{}_2)$.[16,17]

$$2\,1^{\bullet-} \overset{K_{disp}}{\rightleftharpoons} 1 + 1^{2-} \tag{9}$$

$$K_{disp} = \frac{[1][1^{2-}]}{[1^{\bullet-}]^2} \tag{10}$$

In cyclic voltammetry studies of 1, $1^{\bullet-}$ is generated from heterogenous reduction of 1 or by a homogeneous conproportionation reaction between electrochemically generated 1^{2-} and 1. Other than this feature, the reaction proceeds by the general mechanism presented in Scheme I. When the ETC catalytic reaction is initiated at an electrode, the substituted radical anion is produced at a potential more positive than its reduction potential and a competition exists between heterogeneous oxidation of the substituted product (destroying the chain carrier) and propagation of the radical in solution. For the case of 1, the radical must be effectively propagated into solution, given the efficiency of the ETC initiation by cyclic voltammetry. The observed selectivity of the substitution reactions, which results in the sequential formation of mono-substituted and then bis-substituted clusters, must arise from the fact that the homogeneous electron transfer reaction (eq 3) is faster than further substitutions on $M_xL^{\bullet-}$ until M_xL builds up in bulk solution.

It is instructive to compare the voltammetry observed in the reductive ETC catalytic reaction of 1 with that observed for the oxidatively induced $P(OMe)_3$ substitution reactions of the reduced cluster $[BzMe_3N]_2[1^{2-}]$ in CH_3CN solution (Figure 3). Upon an anodic scan from −1.6 V, no oxidation wave is observed for substituted products until passing through the anodic wave for 1^{2-}. On the cathodic scan, the peak current for 1 is smaller than that for 1^{2-} and cathodic peaks are observed for *both* mono- and bis-substituted products. The active radical, $1^{\bullet-}$, is generated by heterogeneous oxidation of 1^{2-} or by a homogeneous conproportionation reaction between 1 in the vicinity of the electrode and bulk 1^{2-}. $1^{\bullet-}$ reacts with PR_3 to produce $11^{\bullet-}$, which can be heterogeneously oxidized at the electrode or homogeneously oxidized by 1 to produce more $1^{\bullet-}$. Thus propagation takes place in the vicinity of the electrode but not into the bulk solution containing 1^{2-}. On the cathodic scan, at potentials near or more negative than $E_{1/2}(11/11^{2-})$, the active radical, $11^{\bullet-}$, is generated by heterogeneous reduction of 11 or by a homogeneous conproportionation reaction between 11^{2-} and bulk 11. No thermodynamically favorable electron transfer reactions are available for $11^{\bullet-}$ (unlike the situation with bulk 1 in solution), and $11^{\bullet-}$ undergoes further substitution to produce $21^{\bullet-}$, which can be heterogeneously or homogeneously oxidized. A steady-state CV is obtained after one cycle. A unique feature of this system is that the same active radical can be generated from an oxidation or a reduction reaction; the observed differences in the voltammetry are a consequence of the species in the bulk solution.

The efficiency of an ETC reaction can be gauged by the turnover number[18] (TN). An estimate of the TN for reaction of 1 with $P(OMe)_3$ is obtained by reducing a bulk solution of 1 at −0.88 V in CH_3CN by 6×10^{-4} faraday in the presence of 100 equiv of added ligand. The substitution reaction proceeds 60% to completion as judged by quantitative IR spectroscopy after a period of 11 min, corresponding to a TN ≈ 1000 mol/faraday. Many other metal carbonyl cluster systems display TN's on the order of 10–100 mol/faraday.[3a] The efficiency of the 1 → 11 chain reaction in comparison to the chains in similar systems may be a consequence of the fact that most of the electrons added to 1 are "stored" in the form of the stable 50-electron cluster 1^{2-}. When radical in solution is removed by a termination reaction, more radical is generated by a conproportionation reaction between 1 and 1^{2-}. Thus, over the course of the reaction, 1^{2-} acts as a fresh source of radical. The TN for the second substitution reaction was measured under the same conditions after reducing at −1.1

---

[16] Equation 11 relates the disproportionation constant to the difference between the 1-e⁻ potentials.

$$\Delta E_{1/2} \approx \Delta E^{\circ\prime} = E^{\circ\prime}{}_2 - E^{\circ\prime}{}_1 = (RT/nF)\ln K_{disp} \tag{11}$$

[17] (a) Richardson, D. E.; Taube, H. *Inorg. Chem.* **1981**, *20*, 1278. (b) Myers, R. L.; Shain, I. *Anal. Chem.* **1969**, *41*, 980. (c) Hinkelmann, K.; Heinze, J. *Ber. Bunsen-Ges. Phys. Chem.* **1987**, *91*, 243.

[18] Turnover number = number of moles of product per faraday.

Table III. ^{1}H NMR Data for Bicapped Triiron Clusters[a,b]

compound	$\delta(C_5H_5)$	$\delta(PR_3)$
$Fe_3(CO)_9(\mu_3\text{-}PMn(CO)_2Cp)_2$ (**1**)	5.05 (d, 2.1)	
$Fe_3(CO)_8[P(OMe)_3](\mu_3\text{-}PMn(CO)_2Cp)_2$ (**11**)	5.01 (d, 1.9, 10H)	3.71 (d, 11.4, 9H)
$Fe_3(CO)_7[P(OMe)_3]_2(\mu_3\text{-}PMn(CO)_2Cp)_2$ (**21**)	4.99 (d, 1.9, 10H)	3.66 (d, 11.1, 18H)
$Fe_3(CO)_8(PMe_3)(\mu_3\text{-}PMn(CO)_2Cp)_2$ (**12**)	5.02 (d, 1.9, 10H)	1.51 (d, 10.2, 9H)
$Fe_3(CO)_7(PMe_3)_2(\mu_3\text{-}PMn(CO)_2Cp)_2$ (**22**)	5.00 (d, 1.8, 10H)	1.48 (d, 9.8, 18H)

[a] NMR spectra recorded in CD_3CN. [b] Chemical shifts are reported in ppm and J_{PH} in Hz (in parentheses).

Table IV. $^{31}P\{^1H\}$ NMR Data for Bicapped Triiron Clusters[a–c]

compound	$\delta(\mu_4\text{-}P)$	$\delta(PR_3)$
$Fe_3(CO)_9(\mu_3\text{-}PMn(CO)_2Cp)_2$ (**1**)	738.0	
$Fe_3(CO)_8[P(OMe)_3](\mu_3\text{-}PMn(CO)_2Cp)_2$ (**11**)	750.6	160.2
$Fe_3(CO)_7[P(OMe)_3]_2(\mu_3\text{-}PMn(CO)_2Cp)_2$ (**21**)	759.6	161.7
$Fe_3(CO)_8(PMe_3)(\mu_3\text{-}PMn(CO)_2Cp)_2$ (**12**)	752.6	14.1
$Fe_3(CO)_7(PMe_3)_2(\mu_3\text{-}PMn(CO)_2Cp)_2$ (**22**)	759.2	10.9

[a] ^{31}P NMR chemical shifts are referenced to a $P(OMe)_3$ external standard ($\delta = 140.0$ ppm). [b] NMR spectra recorded in THF. [c] Chemical shifts are reported in ppm.

V. The calculated turnover number of 100 mol/faraday is considerably smaller than that for the first step, likely as a result of the reduced stability of the PR_3-substituted radical.

Characterization of the PR_3-Substituted Products. The PR_3-substituted products can be obtained on a preparative scale using a catalytic amount of sodium benzophenone ketyl to initiate the radical chain in tetrahydrofuran solution. Mono-substituted **11** and **12** are obtained in reactions where 1 equiv of PR_3 is employed, while bis-substituted **21** and **22** are produced when 2 (or greater) equiv of PR_3 are employed. The substituted products were characterized by ^{31}P, ^{1}H, and ^{13}C NMR spectroscopies in addition to infrared spectroscopy. A singlet is observed in the ^{31}P NMR for the μ_4-P atoms in **1** (δ 738 ppm) as well as for monosubstituted **11** and **12** (δ ~750 ppm) and bis-substituted **21** and **22** (δ ~760 ppm), consistent with replacement of Fe-bound carbonyl ligands as opposed to carbonyl ligands bound to the pendant $CpMn(CO)_2$ groups. Only a single PR_3 resonance is observed for both the mono- and bis-substituted clusters. Integration of the ^{1}H NMR resonance for the C_5H_5 group versus the Me resonances in the PMe_3 or $P(OMe)_3$ ligands confirms the product stoichiometry. ^{1}H and ^{31}P data are collected in Tables III and IV, respectively.

^{13}C NMR spectra were taken on PR_3-substituted clusters that were enriched to ~10% ^{13}CO by stirring a solution of the parent cluster **1** and a catalytic amount of sodium benzophenone ketyl under an atmosphere of ^{13}CO. Enrichment of both the Fe-bound and Mn-bound CO ligands is observed. For **1**, the broad downfield resonance at δ 227.8 ppm ($J_{PC} = 25$ Hz) is assigned to the Mn-bound CO ligands, while the peak at δ 208.6 ppm is assigned to the Fe-bound CO ligands. The fact that only a single resonance is observed for the Fe-bound CO ligands is consistent with rapid turnstile rotation equilibrating the three CO ligands bound to a single Fe center, together with rapid rotation about the Mn–P bonds (or exchange of CO ligands between Fe atoms). Mono-substituted **11** and **12** both display a 2:6 pattern of resonances for the Fe-bound CO ligands. The resonance of intensity 2, assigned to the substituted $Fe(PR_3)(CO)_2$ group, is shifted downfield by ~5 ppm from the $Fe(CO)_3$ resonance in **1**, and coupling to phosphorus is observed ($J_{PC} = 21$ Hz for **11**). The resonances for the unsubstituted $Mn(CO)_2$ and $Fe(CO)_3$ groups are shifted only ~1.5 ppm downfield from the resonances in **1**. Bis-substituted **21** and **22** show a 4:3 pattern of resonances for the Fe-bound CO ligands, definitively establishing that PR_3 substitution has occurred on two different Fe atoms. For **21**, phosphorus coupling ($J_{PC} = 17$ Hz) is observed for the resonance of intensity 4. ^{13}C NMR data are collected in Table V.

Mechanism of the Substitution Reaction. The mechanisms by which a number of cluster systems undergo ligand substitution reactions by an ETC-catalyzed pathway have been studied. The bicapped 50-electron clusters (with two Fe–Fe bonds) $Fe_3(CO)_9(\mu_3\text{-}E)_2$ (E = PPh, NPh, S, Se) rapidly undergo substitution of CO for PR_3 after passing a catalytic amount of cathodic current.[5d] Two distinct mechanisms of reaction are observed. The E = NPh, S, and Se derivatives all react by a dissociative loss of CO, while the rate-limiting step for substitution on the bicapped phosphinidene cluster, $[Fe_3(CO)_9(\mu_3\text{-}PPh)_2]^{\bullet-}$, is isomerization of one μ_3-PPh cap to a μ_2-PPh^-, ligand (eq 12).[5c] Dissociative loss of CO from the radical anion has also been proposed as the mechanism by which the clusters $Co_3(CO)_9(\mu_3\text{-}CR)$[6] and $Co_4(CO)_{10}(\mu_4\text{-}PR)_2$[7] undergo ligand substitution reactions.

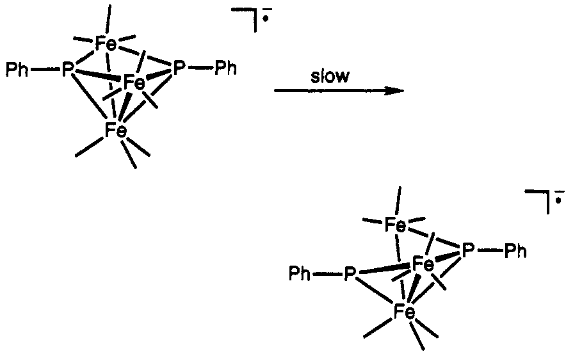

(12)

The question of whether ligand substitution reactions of the active radical $1^{\bullet-}$ (Scheme I, eq 2) occur by an associative or dissociative mechanism is of interest. Extended Hückel calculations show that the LUMO of **1** is an in-plane Fe–Fe antibonding orbital (see **I**). Upon

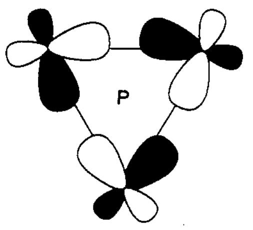

I

introduction of electrons into this orbital, relief of the antibonding interactions can be achieved by a uniform expansion of the Fe_3 triangle or by elongation of a single Fe–Fe edge. It is clear that in the 2-e⁻-reduced product, 1^{2-}, the most stable configuration results from cleavage of a single Fe–Fe bond;[11] the structure adopted by the 1-e⁻-reduced product, $1^{\bullet-}$, is not known. With Fe–Fe bond

Table V. $^{13}C\{^1H\}$ NMR Data for Bicapped Triiron Clusters[a,b]

compound	δ(Mn(CO)$_2$)	δ(Fe(CO)$_3$)	δ(Fe(CO)$_2$(PR$_3$))	δ(C$_p$)	δ(PR$_3$)
$Fe_3(CO)_9(\mu_3\text{-}PMn(CO)_2Cp)_2$ (**1**)	227.8 (d, 25)	208.6		87.0	
$Fe_3(CO)_8[P(OMe)_3](\mu_3\text{-}PMn(CO)_2Cp)_2$ (**11**)	229.2 (d, 21)	210.3 (6C)	213.6 (d, 21, 2C)	86.3	54.8
$Fe_3(CO)_7[P(OMe)_3]_2(\mu_3\text{-}PMn(CO)_2Cp)_2$ (**21**)	230.5 (d, 21)	211.8 (3C)	215.4 (d, 17, 4C)	85.5	54.2
$Fe_3(CO)_8(PMe_3)(\mu_3\text{-}PMn(CO)_2Cp)_2$ (**12**)	228.9 (d, 22)	209.6 (6C)	213.0 (br, 2C)	85.4	21.8 (d, 22)
$Fe_3(CO)_7(PMe_3)_2(\mu_3\text{-}PMn(CO)_2Cp)_2$ (**22**)	230.8 (d, 22)	212.0 (3C)	216.2 (br, 4C)	85.1	21.5 (d, 31)

[a] Chemical shifts are reported in ppm and J_{PC} in Hz (in parentheses). [b] NMR spectra were recorded in CD_2Cl_2.

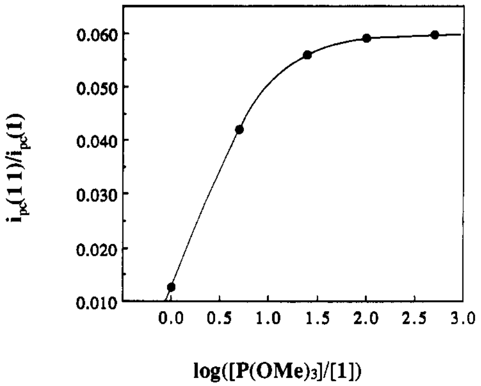

Figure 4. Dependence of the rate of the 1 → 11 conversion on $[P(OMe)_3]$ in 0.1 M $[(n\text{-}Bu)_4N][BF_4]/CH_3CN$ as assessed by the ratio of cathodic peak heights, $i_{pc}(11)/i_{pc}(1)$, observed in the first cyclic voltammogram scan at a scan rate of 50 mV s^{-1}. 1 has a fixed concentration of 2.0 mM.

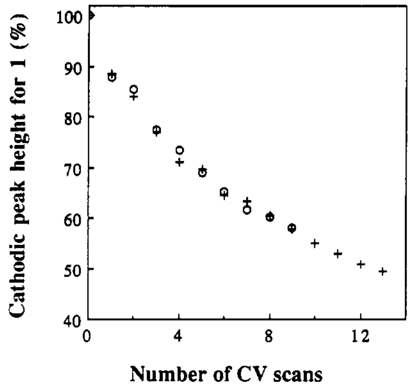

Figure 5. Decrease in the cathodic peak height of the reactant, 1 (2.0 mM), as a function of the number of cyclic voltammogram scans (scan rate = 50 mV s^{-1}) in the presence of 5 equiv of PR_3 in 0.1 M $[(n\text{-}Bu)_4N][BF_4]/CH_3CN$. Data for $P(OMe)_3$ (O) and PMe_3 (+) are shown.

cleavage as a readily available degree of freedom for relief of excess electrons in this system, an associative mechanism for ligand substitution, proceeding through a 51-electron transition state (or intermediate), is a plausible reaction pathway. Ligand addition reactions of metal clusters accompanied by metal–metal bond scission to form stable products with two additional electrons have been observed in many systems.[19]

To experimentally address the mechanism of the ligand substitution reaction, the kinetics of the ETC reaction of $1^{\bullet -}$ were monitored by cyclic voltammetry as a function of PR_3 ligand and the ligand concentration.[20] The ratio of the product cathodic peak current to the reactant cathodic peak current ($i_{pc}(11)/i_{pc}(1)$) was measured from the initial scan in a series of cyclic voltammograms as a function of the concentration of added $P(OMe)_3$ (Figure 4). At $[P(OMe)_3]/[1] > 25$, the amount of substituted product formed is invariant to $P(OMe)_3$ concentration. Moreover, the rates of ligand substitution for PMe_3 and $P(OMe)_3$ under identical conditions, as assessed by measurement of the cathodic peak current for 1 as a function of number of CV scans, are essentially identical (Figure 5). The insensitivity of the ligand substitution kinetics to the concentration and nature of the incoming phosphorus nucleophile is inconsistent with an associative substitution mechanism and implies that the ligand substitution reaction occurs after the rate-limiting step.

A marked dependence of the reaction rate on [CO] is evident in cyclic voltammograms taken under a CO atmosphere in the presence of PR_3 (Figure 6a). The ETC reaction is essentially shut down when the solution containing 1 and 5 equiv of $P(OMe)_3$ is placed under 1 atm of CO. When a vacuum is applied to the same solution to remove CO, the catalytic cycle resumes (Figure 6b). The observed qualitative [CO] and [L] dependences could be consistent with either a CO-dissociative mechanism *or* an intramolecular rearrangement to a coordinatively unsaturated intermediate via M–M or M–P bond cleavage (such as that observed for $[Fe_3(CO)_9(\mu_3\text{-}PPh)_2]^{\bullet -}$). On the basis of the observation of facile ligand interchange reactions for the **1n** clusters in the *absence* of added ligand (see below), we favor a CO-dissociative pathway (eqs 13 and 14).[21] At sufficiently high concentrations of PR_3, back-reaction with CO cannot compete with trapping by PR_3; however under a CO atmosphere, the unsaturated species[22] $1a^{\bullet -}$ is efficiently trapped by CO so the reaction does not proceed. The proposed electrocatalytic ligand substitution mechanism for the production of mono- and bis-substituted clusters is summarized in Scheme II.

$$\underset{49\ e^-,\ 1^{\bullet -}}{[Fe_3(CO)_9(\mu_3\text{-}PMn(CO)_2Cp)_2]^{\bullet -}} \underset{k_{-1}}{\overset{k_1}{\rightleftharpoons}} \underset{47\ e^-,\ 1a^{\bullet -}}{[Fe_3(CO)_8(\mu_3\text{-}PMn(CO)_2Cp)_2]^{\bullet -}} + CO \quad (13)$$

$$1a^{\bullet -} + PR_3 \xrightarrow{k_2} \underset{11^{\bullet -},\ R = OMe;\ 12^{\bullet -},\ R = Me}{[Fe_3(CO)_8(PR_3)(\mu_3\text{-}PMn(CO)_2Cp)_2]^{\bullet -}} \quad (14)$$

The voltammetry is qualitatively the same in CH_2Cl_2 as in CH_3CN solution, implying that coordination of solvent does not play an important role in the reaction. In THF solution, however, considerably more substitution takes place in the first CV scan ($i_{pc}(11)/i_{pc}(1) \approx 1$) than in either CH_3CN or CH_2Cl_2 solution. The rate of the substitution

---

(19) Vahrenkamp, H. *Adv. Organomet. Chem.* **1983**, *22*, 169.

(20) Obtaining quantitative information about the rate of CO substitution using digital simulation techniques for the case of a composite 2-e$^-$ wave would require independent information about each one-electron step.

(21) It is interesting to note that the small CO character in the predominantly Fe–Fe antibonding LUMO of 1 is M–CO bonding.

(22) The numbering scheme for the coordinatively unsaturated radical is derived from adding a to the abbreviation for the parent cluster radical with one additional CO ligand.

Scheme II

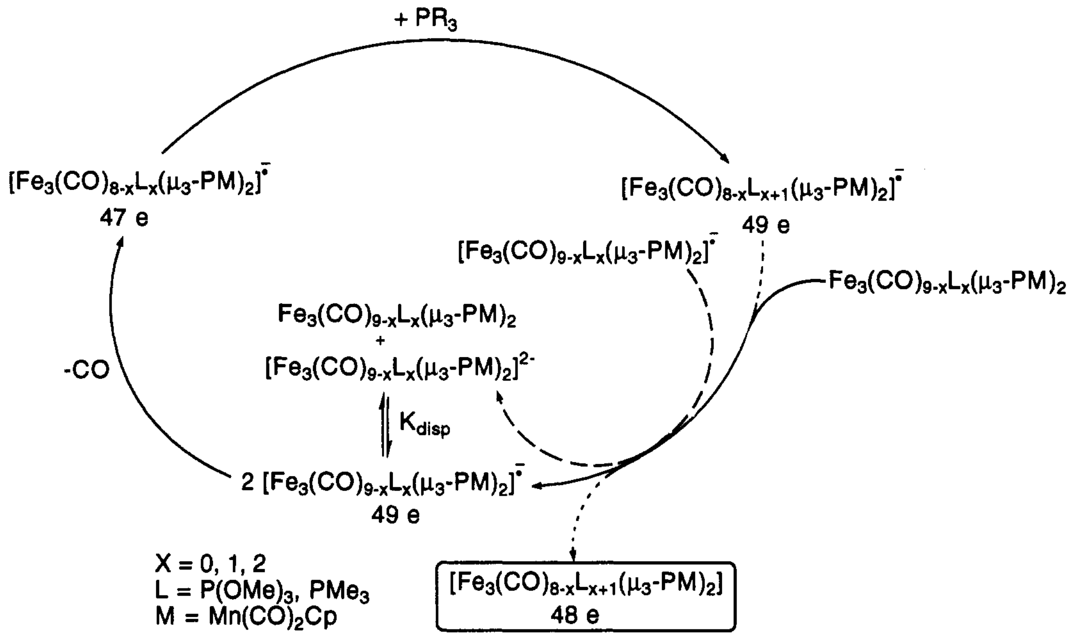

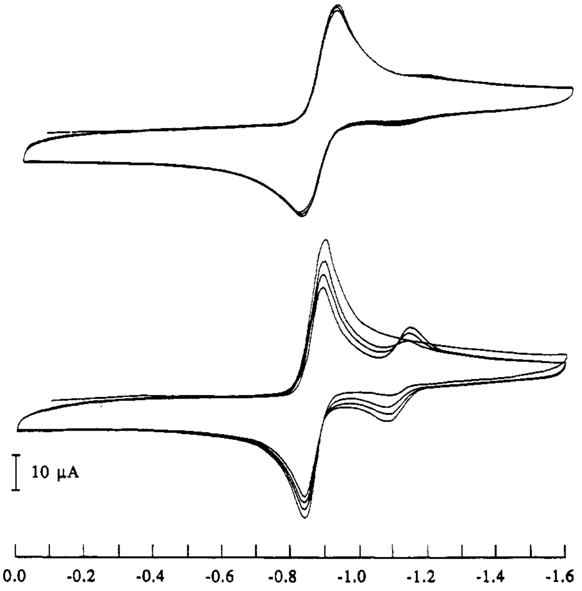

Figure 6. Successive cyclic voltammograms (scan rate = 50 mV s^{-1}) of **1** (0.7 mM) in 0.1 M [(n-Bu)$_4$N][BF$_4$]/CH$_3$CN containing 5 equiv of P(OMe)$_3$ (a, top) under 1 atm of CO and (b, bottom) after CO is removed by applying vacuum.

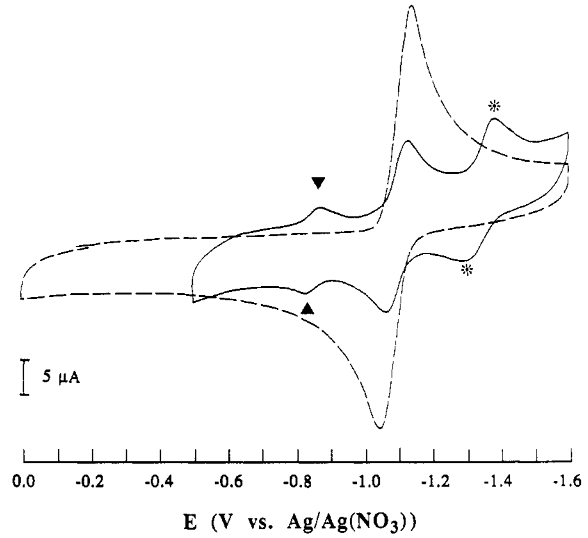

Figure 7. Cyclic voltammograms (scan rate = 50 mV s^{-1}) of an isolated sample of **11** (0.80 mM) in 0.1 M [(n-Bu)$_4$N][BF$_4$]/CH$_3$CN (dashed line) and after passing 2 faradays in a bulk electrolysis experiment at E = 1.1 V (solid line); waves for **1**/**1**$^{2-}$ and **21**/**21**$^{2-}$ are marked.

reaction is directly proportional to the concentration of the radical, and the observed difference in voltammetry is a consequence of the fact that the disproportionation constant is smaller in THF solution than in the other solvents.

The results of bulk electrolysis experiments on the PR$_3$-substituted clusters provide evidence for the ligand-loss pathways proposed above. On the cyclic voltammetry time scale, isolated pure samples of the mono- and bis-substituted clusters are stable, and there is no evidence of decomposition in the CV (see Figure 7 for **11**). However, we were not able to prepare pure samples of dinegatively charged substituted clusters by bulk reduction. A CV taken after passing current corresponding to ~2 faradays (at E = −1.15 V) to a solution of **11** shows redox couples for **1**, **11**, and **21** (Figure 7), presumably corresponding to **1**$^{2-}$, **21**, and **11**$^{2-}$ present in solution. Some decomposition products also deposit on the electrode during the course of the electrolysis. A chemical reduction reaction provided insight into the chemistry taking place during bulk reduction. Reaction of the monosubstituted clusters, **11** and **12**, with 1 equiv of Cp$_2$Co in acetonitrile solution results in a clean ligand redistribution reaction to produce ~$^1/_2$ equiv of **1**$^{2-}$ and ~$^1/_2$ equiv of the bis-PR$_3$ cluster (as determined by ^{31}P NMR spectroscopy) after stirring for 30 min, together with a small amount of decomposition products (eq 15). The net reaction corresponds to a

$$[\mathrm{Fe_3(CO)_8(PR_3)(\mu_3\text{-}PMn(CO)_2Cp)_2}] + 1e^- \rightarrow {}^1/_2[\mathrm{Fe_3(CO)_9(\mu_3\text{-}PMn(CO)_2Cp)_2}]^{2-} + {}^1/_2[\mathrm{Fe_3(CO)_7(PR_3)_2(\mu_3\text{-}PMn(CO)_2Cp)_2}] \quad (15)$$

disproportionation reaction of the radical **1n**$^{\bullet-}$, which is

Scheme III

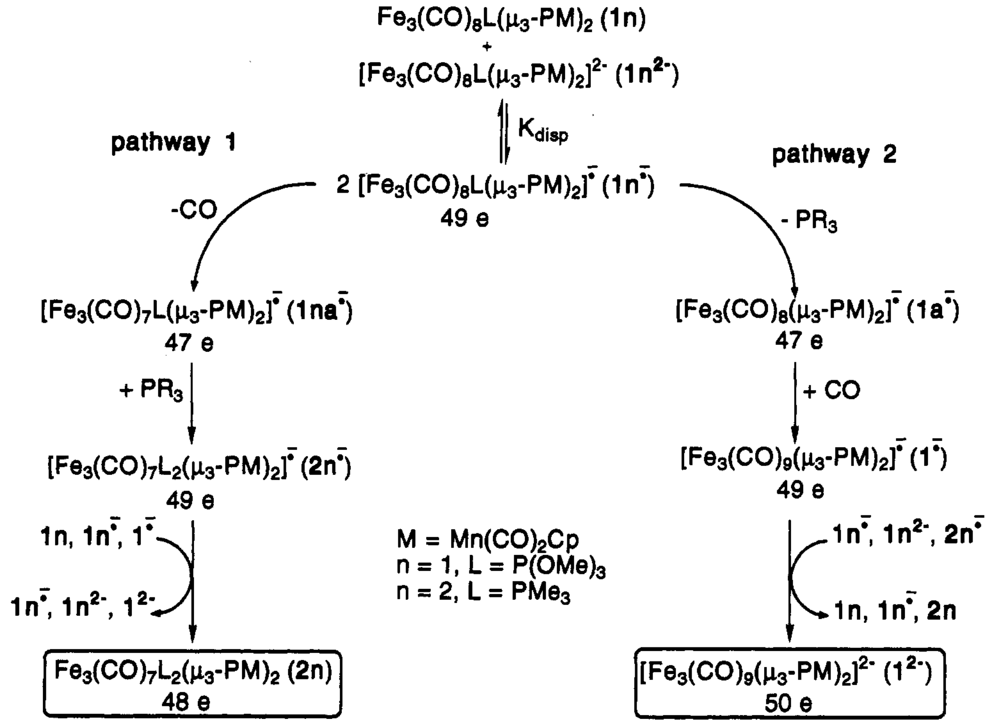

induced by the redistribution of the PR_3 ligands.[23] In the bulk reduction of **1n**, the radical $\mathbf{1n}^{\bullet-}$ has two possible fates: loss of CO or loss of PR_3 (Scheme III). After CO loss (pathway 1), if $\mathbf{1na}^{\bullet-}$ reacts with liberated PR_3, the resulting bis-substituted radical $\mathbf{2n}^{\bullet-}$ is capable of reducing **1n**, $\mathbf{1n}^{\bullet-}$, or $\mathbf{1}^{\bullet-}$ to produce **2n**; **2n** will not participate further in reactions. Likewise, after PR_3 loss (pathway 2), if $\mathbf{1a}^{\bullet-}$ is trapped by CO present in solution to generate $\mathbf{1}^{\bullet-}$, reduction of $\mathbf{1}^{\bullet-}$ by $\mathbf{1n}^{\bullet-}$, $\mathbf{1n}^{2-}$, or $\mathbf{2n}^{\bullet-}$ to produce the stable product, $\mathbf{1}^{2-}$, is a thermodynamically favored reaction. Once $\mathbf{1}^{2-}$ is formed, it will also not participate in further reactions. Because the only sources of CO or PR_3 are the ligand-loss reactions, the reactions of the coordinatively unsaturated radicals with ligands must be quite efficient.

In the detailed study of the electrochemical behavior of $Co_3(CO)_{9-x}L_x(\mu_3\text{-}CR)$ clusters, ligand redistribution reactions similar to those observed for the mono-substituted clusters were evident on the cyclic voltammetry time scale.[6a] For this series of cobalt clusters, as the degree of phosphine substitution increases, the lability of the M–CO bonds decreases (due to increased π-back-bonding between CO and the more electron-rich metal centers), and upon reduction to the labile radical anion, PR_3 loss becomes more favored over CO loss. After loss of PR_3 from the radical, the coordinatively unsaturated 47-electron radical-anion product is more easily reduced than the starting cluster, and reduction to a 48-electron dianion takes place (ECE mechanism). A peak for oxidation of the 48-electron dianion is observed in the CV.

The analysis presented above regarding the ligand redistribution reaction observed for the **1n** clusters did not consider reduction of the coordinatively unsaturated radical anion, $\mathbf{1a}^{\bullet-}$, and no redox couples that could not be assigned were observed in the bulk reduction experiment. It is possible that in this system (1) the $\mathbf{1a}^{\bullet-}/\mathbf{1a}^{2-}$ reduction potential lies negative of the $\mathbf{1n}/\mathbf{1n}^{\bullet-}$ and $\mathbf{1n}^{\bullet-}/\mathbf{1n}^{2-}$ potentials or (2) reaction of $\mathbf{1a}^{\bullet-}$ with CO or PR_3 is competitive with reduction and the 48-electron dianions are not stable, leading to decomposition. In bulk reduction experiments on bis-substituted clusters, more extensive decomposition is observed than for the monosubstituted clusters. On the basis of the results for the $Co_3(CO)_{9-x}L_x(\mu_3\text{-}CR)$ clusters, loss of PR_3 (eq 16) from $\mathbf{2n}^{\bullet-}$

$$\underset{\mathbf{2n}^{\bullet-}}{[Fe_3(CO)_7(PR_3)_2(\mu_3\text{-}PMn(CO)_2Cp)_2]^{\bullet-}} \rightleftharpoons \underset{\mathbf{1na}^{\bullet-}}{[Fe_3(CO)_7(PR_3)(\mu_3\text{-}PMn(CO)_2Cp)_2]^{\bullet-}} + PR_3 \quad (16)$$

should be a more favored reaction pathway than for $\mathbf{1n}^{\bullet-}$. The observed decomposition could result from reduction of $\mathbf{1na}^{\bullet-}$ by $\mathbf{2n}^{\bullet-}$. Additionally, in the event of CO loss from $\mathbf{2n}^{\bullet-}$, formation of a stable tris-substituted cluster is not a possible reaction.

Summary and Conclusions

The substitutionally labile radical $[Fe_3(CO)_9(\mu_3\text{-}PMn(CO)_2Cp)_2]^{\bullet-}$ ($\mathbf{1}^{\bullet-}$) is the 1-e$^-$-reduced intermediate in an overall 2-e$^-$ process relating the inert complexes $Fe_3(CO)_9(\mu_3\text{-}PMn(CO)_2Cp)_2$ and $[Fe_3(CO)_9(\mu_3\text{-}PMn(CO)_2Cp)_2]^{2-}$. The concentration of the active radical in solution is governed by the value of the disproportionation constant, $K_{disp}(\mathbf{1}^{\bullet-})$. $\mathbf{1}^{\bullet-}$ undergoes electron transfer chain catalytic substitution of CO for PR_3 on two different $Fe(CO)_3$ groups to sequentially produce mono- and then bis-substituted products. The two-electron behavior observed for **1** is maintained in the PR_3-substituted derivatives. The substitution reaction occurs after the rate-determining step, and a mechanism involving elimination of CO from the radical anion is proposed. The PR_3-substituted radicals are unstable to bulk electrolysis.

---

[23] Catalytic disproportionation reactions of M–M-bonded dimers can be initiated photochemically or reductively: (a) Tyler, D. R. *Prog. Inorg. Chem.* **1988**, *36*, 125. (b) Stiegman, A. E.; Tyler, D. R. *J. Am. Chem. Soc.* **1985**, *107*, 967. (c) Stiegman, A. E.; Tyler, D. R. *Inorg. Chem.* **1984**, *23*, 527. (d) Goldman, A. S.; Tyler, D. R. *J. Am. Chem. Soc.* **1986**, *108*, 89. (e) Goldman, A. S.; Tyler, D. R. *J. Am. Chem. Soc.* **1984**, *106*, 4066. (f) Stiegman, A. E.; Stieflitz, M.; Tyler, D. R. *J. Am. Chem. Soc.* **1983**, *105*, 6032.

Reaction of the monosubstituted cluster, $Fe_3(CO)_8(PR_3)(\mu_3\text{-}PMn(CO)_2Cp)_2$, with 1 equiv of reducing agent results in an efficient ligand redistribution reaction to produce 0.5 equiv of each of the bis-substituted cluster, $Fe_3(CO)_7(PR_3)_2(\mu_3\text{-}PMn(CO)_2Cp)_2$, and the unsubstituted dianion, 1^{2-}. This redistribution reaction is efficient because the bis-PR_3-substituted radical is the best reducing agent in the system and the unsubstituted radical is the most easily reduced species.

Experimental Section

Materials and General Procedures. All reactions were performed under an atmosphere of prepurified dry nitrogen using standard Schlenk and syringe techniques. Reagent grade solvents were distilled from the appropriate drying agent under nitrogen before use.[24] Solids were manipulated in a Vacuum Atmospheres drybox equipped with a recirculator and Dri-Train system. Cobaltocene and the ligands $P(OMe)_3$ and PMe_3 were purchased from Strem Chemicals and used as received. Carbon monoxide gas was purified by passing through a column containing oxygen scavenger (BAS) and 4-Å molecular sieves before use. The cluster $Fe_3(CO)_9(\mu_3\text{-}PMn(CO)_2Cp)_2$ (1) was prepared by following a literature procedure.[15] The cluster $(BzMe_3N)_2[Fe_3(CO)_9(\mu_3\text{-}PMn(CO)_2Cp)_2]$ was prepared by a procedure analogous to that for the $[(Ph_3P)_2N]^+$ salt.[11] Elemental analyses were performed by Mikroanalytisches Labor Pascher, Remagen-Bandorf, Germany.

Spectroscopic Measurements. IR spectra were recorded on a BOMEM Michelson 120 FT-IR spectrometer in solution using CaF_2-windowed cells. NMR spectra were recorded on Bruker AC-200, Bruker AMX-300, and Varian XL-400 spectrometers. $Cr(acac)_3$ (acac = acetylacetonate) was employed as a relaxation agent for all ^{13}C NMR samples. ^1H and ^{13}C NMR spectra were referenced to the solvent resonances. ^{31}P NMR samples were referenced to an external sample of $P(OMe)_3$ (δ 140.0 ppm) contained in a concentric tube.

Electrochemical Measurements. Electrochemical experiments were performed with a Princeton Applied Research Model 273 potentiostat/galvanostat equipped with a Yokogawa 3025 X-Y recorder. Cyclic voltammograms were observed on solutions in a single-compartment airtight three-electrode cell under nitrogen using positive-feedback *iR* compensation. A glassy-carbon working electrode (area = 7.5 mm^2) and a Pt-wire counter electrode were employed. Bulk reduction experiments employed both a Pt-mesh working electrode and a glassy-carbon electrode. In acetonitrile solutions, the potential was referenced to a Ag/0.1 M $AgNO_3$ reference electrode, which was separated from the analyte solution by placement in a Vycor-glass-tipped compartment. The potential for the standard Cp_2Fe/Cp_2Fe^+ couple ($E_{1/2}$ = 0.420 V vs Ag/0.1 M $AgNO_3$) was used to convert all of the potentials in this paper to the Ag/0.1 M $AgNO_3$ reference.

Synthesis of $Fe_3(CO)_8(PR_3)(\mu_3\text{-}PMn(CO)_2Cp)_2$ (1n). A solution of sodium benzophenone ketyl was prepared by dissolving sodium (0.1 g, 4.3 mmol) and benzophenone (0.1 g, 0.55 mmol) in 5 mL of THF.[25] A sample of 1 (20 mg, 0.024 mmol) in THF (5 mL) was reduced by adding 5 μL of the sodium benzophenone ketyl solution in the presence of 1 equiv of PR_3. Infrared spectroscopy after 2 min of stirring showed quantitative conversion to the mono-substituted derivatives **1n** (n = 1, L = $P(OMe_3)$; n = 2, L = PMe_3). The solvent was removed under vacuum, the residue was dissolved in CH_2Cl_2, and the solution was layered with hexanes to yield purple-brown crystals. Typical isolated yields: 40–70%. Anal. Calcd (found) for $Fe_3Mn_2P_3C_{25}O_{15}H_{19}$ (**11**): C, 32.30 (32.24); H, 2.06 (2.05).

Synthesis of $Fe_3(CO)_7(PR_3)_2(\mu_3\text{-}PMn(CO)_2Cp)_2$ (2n). Bis-substituted clusters were prepared by chemical reduction of 1 or monosubstituted **1n**. A 20-mg sample of 1 or **1n** was reduced by adding 5 μL of sodium benzophenone ketyl solution in the presence of the required quantitative amount of PR_3. Infrared spectroscopy after 20 min of stirring showed quantitative conversion to the bis-substituted derivatives, **2n** (n = 1, L = $P(OMe_3)$; n = 2, L = PMe_3). The solvent was removed under vacuum, the residue was dissolved in CH_2Cl_2, and the solution was layered with hexanes to yield purple-brown crystals. Typical isolated yields: 30–50%. Anal. Calcd (found) for $Fe_3Mn_2P_4C_{27}O_{17}H_{28}$ (**21**): C, 31.61 (31.41); H, 2.75 (2.82).

Chemical Reduction of 11 and 12. A standard solution of Cp_2Co (13 mM) was prepared in CH_3CN, and 1.1 equiv of the cobaltocene solution was added to a 5-mg solid sample of **11** or **12**. The solution was rapidly stirred for 10 min before analysis by infrared and ^{31}P NMR spectroscopy.

Acknowledgment. Partial financial support was provided by a Presidential Young Investigator Award from the National Science Foundation (CHEM-8958027).

OM930657B

---

(24) Gordon, A. J.; Ford, R. A. *The Chemist's Companion*; Wiley: New York, 1977.

(25) The first reduction potential of benzophenone in CH_3CN is −2.15 V vs Ag/0.1 M $AgNO_3$.